JOURNAL OF MATERIALS SCIENCE 27 (1992) 3719–3725

Internal pressure test for characterizing fast-fracture reliability of grinding wheels

S. SANTHANAM
Mechanical Engineering Department, Villanova University, Villanova, PA 19085, USA
S. CHANDRASEKAR
School of Industrial Engineering, Purdue University, West Lafayette, IN 47907, USA

A constant danger associated with the use of most grinding wheels (vitrified-bond alumina and silicon carbide wheels) is the possibility of fracture during operation. A standard practice is to subject newly manufactured wheels to a spin test and accept wheels that survive. We propose an internal pressure test which offers a simpler, more economical alternative to the spin test for testing grinding wheels. Probabilities of failure in the internal pressure test are correlated with failure probabilities in the spin test using probabilistic fracture mechanics. Results indicate a reasonably good correlation between the two tests, thus demonstrating their equivalence. A scheme for the easy implementation of the internal pressure test to detect damage in grinding wheels is outlined.

1. Introduction

Vitrified-bond abrasive grinding wheels have been the workhorses of the grinding industry for the last few decades. A typical vitrified-bond wheel consists (in vol %) of about 50 to 70% abrasive particles and 15 to 25% bond material, with voids and cavities comprising the rest. In many grinding processes, the grinding wheel is spun at a high peripheral velocity (~ 20–$40\ m\ s^{-1}$). The operating speeds have generally increased as the strength of the bond has increased. Higher speeds have improved productivity but safety considerations have limited operating speeds. Because of high surface speeds, the disintegration of a grinding wheel during a grinding operation is extremely dangerous and can prove fatal. Like most ceramic materials, abrasive wheels are brittle and unable to deform plastically under load. This results in a significant scatter in fracture strength [1, 2] and this unpredictability is the principal cause of worry.

Grinding wheel fracture is an old problem and efforts have been made on several fronts to tackle it. Historically, the use of stronger bonded wheels and the provision of wheel guards in grinding machines along with conservative spin speeds has been the solution of choice [3]. These are not completely satisfactory ways to solve the problem since they cannot completely eliminate the risk of an accident due to wheel failure. A common test used at the manufacturer's plant as well as the user's workshop is the "ring" test where cracks are detected by monitoring the acoustic tones emitted when the wheel is lightly struck. A "dull" note denotes the presence of one or more cracks and a "clear" note is presumed to be a sign of absence of life-threatening cracks. This method relies on the ability and experience of the individual monitoring the tones. Probably the most crucial test performed to assess the reliability of a grinding wheel is the spin test. The spin test involves rotating wheels to 1.5 times their rated operating speed and categorizing wheels that survive as acceptable [3]. The spin test is a proof test and requires a significant investment in capital equipment. It is usually performed by wheel manufacturers and hardly ever by wheel users. Any damage to the grinding wheel that occurs during handling or transport from the manufacturer to the user is therefore not monitored by this test.

The use of non-destructive techniques has of late been the subject of extensive study. A good discussion of X-radiographic, ultrasonic and resonance techniques for detecting cracks in abrasive wheels can be found in Smith [4]. Attempts have also been made to devise schemes for on-line detection of critical cracks [5, 6]. These schemes have not yet been developed to the stage where they can perform reliably and consistently in a realistic grinding situation.

Non-destructive and in-process crack detection techniques have not gained ground because most manufacturers and users are of the opinion that current practices during manufacture and recommended operating procedures are adequate to ensure the integrity of grinding wheels. The spin test is a principal part of these practices. This paper presents an internal pressure test as an alternative to the spin test for testing grinding wheels. The proposed test is inexpensive and can be performed easily at the user end or at the manufacturers plant.

2. Internal pressure test

Fig. 1 is a schematic diagram of the internal pressure test apparatus that was developed for testing grinding

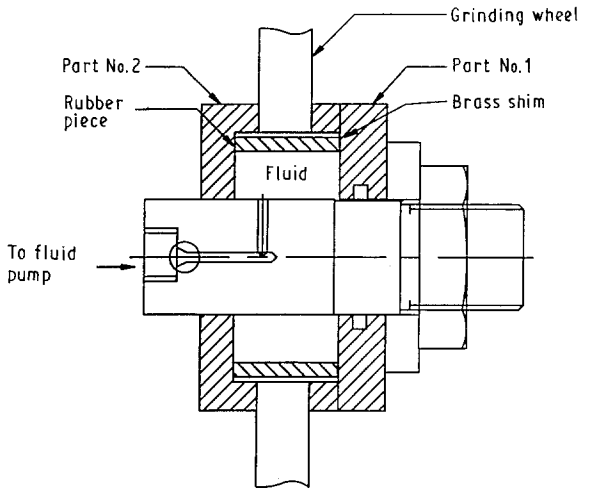

Figure 1 Internal pressure test apparatus.

wheels. The annular bore of the grinding wheel is coated with an epoxy adhesive, the thickness of the epoxy layer being 4 to 5 mm. The wheel is then mounted in the apparatus in a manner that allows pressurization internally from the bore. The pressurizing medium is a liquid such as oil or water. The epoxy coating is necessary to prevent the fluid from coming into direct contact with the hub of the wheel as this causes the fluid to leak out under pressure through the pores in the grinding wheel. The wheel is loaded to a "proof" pressure that is "equivalent" to the maximum speed in the spin test. Wheels that survive are considered acceptable for service. We analyse the mechanics of both the spin and the internal pressure tests and establish an equivalence between the two in the following sections.

Both tests give rise to a biaxial stress situation in the wheel. The stresses in a spinning annular disc are [15]

$$\sigma_t = \rho\omega^2 \frac{3+\mu}{8}\left(r_0^2 + r_i^2 + \frac{r_0^2 r_i^2}{r^2} - \frac{1+3\mu}{3+\mu} r^2\right) \quad (1)$$

$$\sigma_r = \rho\omega^2 \frac{3+\mu}{8}\left(r_0^2 + r_i^2 - \frac{r_0^2 r_i^2}{r^2} - r^2\right)$$

where σ_t is the hoop stress, σ_r is the radial stress, ρ the density, ω the spin speed (rad s^{-1}), μ the Poisson's ratio, and r_i and r_0 are, respectively, the internal and external radii. The corresponding expressions for an annular disc under internal pressure loading are

$$\sigma_t = p\frac{r_i^2}{r_0^2 - r_i^2}\left(1 + \frac{r_0^2}{r^2}\right) \quad (2)$$

$$\sigma_r = p\frac{r_i^2}{r_0^2 - r_i^2}\left(1 - \frac{r_0^2}{r^2}\right)$$

where p is the internal pressure.

Both tests result in tensile hoop stresses which attain a maximum value at the inner radius. But while the spinning disc experiences tensile radial stresses, the wheel with internal pressure loading is subjected to compressive radial stresses which are a maximum at the inner radius. The difference in stress situations prevents direct comparisons of the strength values in the two tests for establishing the desired "proof pressure". Moreover, grinding wheels like most brittle materials exhibit a strength variability as a direct result of the scatter in size distribution of critical strength-controlling flaws. A consequence of this is that specimen size and stress state strongly influence the fracture strength. Hence the strength of these materials cannot be considered a deterministic quantity but must be characterized statistically.

3. Theory

One of the earliest probabilistic approaches used to account for the scatter in fracture strength of brittle materials was introduced by Weibull [7]. Weibull postulated a random distribution of flaws without specifying their size or shape. The Weibull approach, which is based on the weakest-link theory, was given an integral formulation by Vardar and Finnie [8] for a general, non-uniform, multiaxial stress situation where failure is governed by a volumetric flaw distribution:

$$P_f = 1 - \exp\left\{-\int_V \left[K \int_A (\sigma_n)^m \, dA\right] dV\right\} \quad (3)$$

Here P_f is the probability of failure, V the volume of the stressed member, dV a volume element, m the Weibull modulus, σ_n the normal stress and K a constant which will be defined shortly. The formulation considers only the normal tensile stresses acting on all planes at each point in the solid. This leads to the term in square brackets in Equation 3 where the integral is evaluated on the surface of the unit sphere in Fig. 2, only over regions where the normal stress is tensile. The normal stress on the surface of the unit sphere, in terms of the principal stresses and the polar and azimuthal angles, is

$$\sigma_n = \cos^2\phi(\sigma_1 \cos^2\psi + \sigma_2 \sin^2\psi) + \sigma_3 \sin^2\phi \quad (4)$$

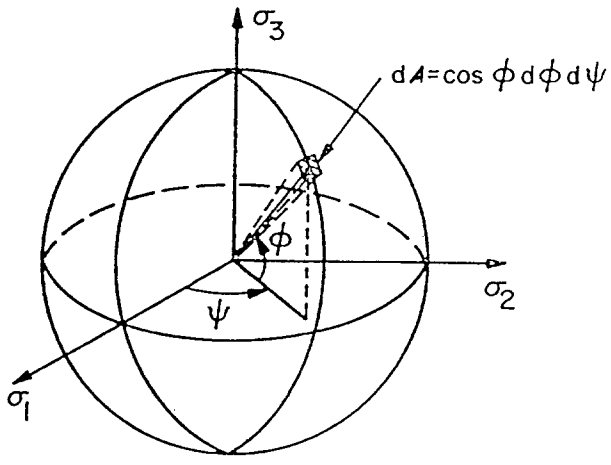

Figure 2 Geometric variables used to describe location on a unit sphere.

The constant K in Equation 3 is given by

$$K = \frac{2m + 1}{2\pi(\sigma_{ov})^m} \quad (5)$$

where m is the Weibull modulus and σ_{ov} the characteristic strength. The $(2m + 1)/2\pi$ term in Equation 5 is a compatibility factor required to make the result of integrating Equation 3 for uniaxial stress cases agree with the results obtained from the one-dimensional Weibull equation

$$P_f = 1 - \exp\left[- \int_V \left(\frac{\sigma}{\sigma_{ov}}\right)^m dV \right] \quad (6)$$

If it is determined that failure of the structure under study originates from surface flaws then the foregoing expressions have to be modified accordingly [9]:

$$P_f = 1 - \exp\left[- \int_S K_s \int_A (\sigma_{ns})^m dA\, dS \right] \quad (7)$$

S is the surface of the body, dS an area element, dA the area element of the curved surface of the unit disc in Fig. 3. The normal stress, σ_n, on the curved surface of the unit disc in terms of the principal stresses is

$$\sigma_n = \sigma_1 \cos^2\psi + \sigma_2 \sin^2\psi \quad (8)$$

The constant K_s is related to m and the characteristic surface flaw strength σ_{os} by

$$K_s = [B(m + 0.5, 0.5)(\sigma_{os})^m]^{-1} \quad (9)$$

where $B(x, y)$ is the beta function.

The Weibull method as described above is intuitively plausible but is a little arbitrary. It does not specify the nature of the flaw causing failure. Batdorf and co-workers [10, 11] have proposed that failure predictions should be based on a combination of the weakest-link approach and linear elastic fracture mechanics (LEFM). The Batdorf theory assumes random flaw orientation and a consistent crack geometry. The combined probability of the critical flaw being within a certain size range and being oriented so that it may cause fracture is calculated. Since flaw sizes correspond to strength levels, the probability of a crack existing within a critical strength range is determined.

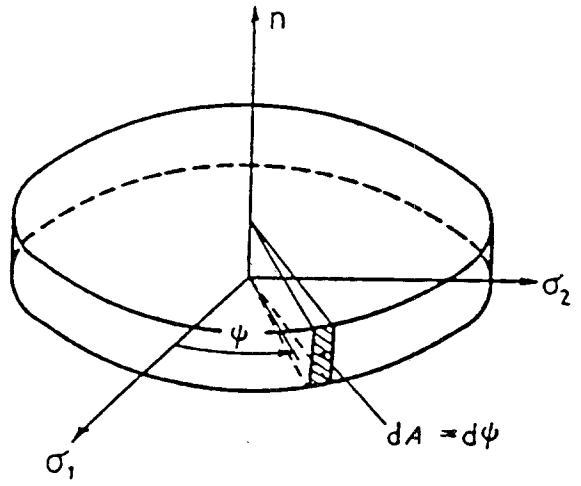

Figure 3 Geometric variables used to describe location on a unit disc.

The component failure probability for volume flaws, P_f, is expressed as

$$P_f = 1 - \exp\left[- \int_V \int_0^{\sigma_{e,max}} \left(\frac{\Omega(\Sigma, \sigma_{cr})}{4\pi}\right) \times \left(\frac{dN_V(\sigma_{cr})}{d\sigma_{cr}}\right) dV\, d\sigma_{cr} \right] \quad (10)$$

where σ_{cr}, the critical stress, is defined as the remote, uniaxial fracture strength of a given crack in mode I loading. The solid angle $\Omega(\Sigma, \sigma_{cr})$ is the sphere of Fig. 2 containing all the crack orientations for which $\sigma_e > \sigma_{cr}$, due to the existing stress state Σ. The effective stress, σ_e, is defined as the equivalent mode I stress on the flaw. $\sigma_{e,max}$ is the maximum effective stress. The Batdorf crack density function, $N_V(\sigma_{cr})$, is approximated by a power function:

$$N_V(\sigma_{cr}) = k_{BV}(\sigma_{cr})^m \quad (11)$$

where the Batdorf volume crack density coefficient k_{BV} and Weibull modulus, m, are evaluated from experimental uniaxial fracture data. Evaluation of the Batdorf coefficient requires a fracture criterion and specification of a crack shape. A shear-insensitive criterion is based on the assumption that fracture occurs when $\sigma_n = \sigma_e > \sigma_{cr}$. Such a criterion leads directly to the Weibull formulation (Equations 3 and 7) for the probability of failure. A shear-sensitive criterion, on the other hand, assumes that a shear stress T, applied parallel to the crack plane in mode II or mode III, also contributes to fracture. In this case the effective stress σ_e is a function of both σ_n and T. The exact form of this function will depend on the fracture criterion and crack shape.

We model the volumetric flaws in grinding wheels as penny-shaped cracks. The fracture criterion that is used in the subsequent analysis is based on strain energy release-rate considerations [11]. The following expression for the effective stress emerges as a result of these assumptions:

$$\sigma_e = \left(\frac{\sigma_n^2 + T^2}{(1 - 0.5\mu)^2}\right)^{0.5} \quad (12)$$

σ_n is given by Equation 4 and the expression for shear stress, T, with reference to Fig. 2 is

$$T = [(\sigma_1 - \sigma_2)^2 l^2 m^2 + (\sigma_2 - \sigma_3)^2 m^2 n^2 + (\sigma_3 - \sigma_1)^2 n^2 l^2]^{0.5} \quad (13)$$

where l, m and n are the direction cosines of the normal to the crack plane.

For fractures originating from surface flaws (half-penny cracks), the Batdorf analysis leads to the following expression for failure probability:

$$P_f = 1 - \exp\left[- \int_A \int_0^{\sigma_{max}} \left(\frac{\Omega(\Sigma, \sigma_{cr})}{2\pi}\right) \times \left(\frac{dN_S(\sigma_{cr})}{d\sigma_{cr}}\right) dA\, d\sigma_{cr} \right] \quad (14)$$

where Ω is the total arc length on a unit radius circle (Fig. 3) for which $\sigma_e > \sigma_{cr}$. The cracks are assumed to be half-penny cracks with planes normal to the surface

and random orientations in the plane of the external boundary. The effective stress, σ_e, is given by Equation 12. The surface crack density function, N_S, is assumed to be of the same form as N_V (Equation 11) with a coefficient k_{BS}.

The standard approach used in failure probability predictions of loaded brittle components is to first characterize the flaw population with simple uniaxial tests (typically four-point bending tests). This flaw population is then used to determine failure probabilities for complex component geometry and loading using the analyses outlined above [12–14].

3. Experimental results and discussion

The vitrified-bond aluminium oxide abrasive wheels that were tested in this study were designated as WA46-I9V9 (Ferro-Electric Corp., Buffalo, New York). A number of rectangular bars (20) were sliced from a random selection of grinding wheels. These bars were then ground to the dimensions of 102 mm $\times$ 12.7 mm $\times$ 12.7 mm. The 20 bar specimens were strength-tested in four-point bending (76.2 mm outer span and 25.4 mm inner span) at a crosshead speed of 0.5 mm min^{-1}. The bending strength (tensile stress at the outermost fibre in the inner span at fracture) data were analysed using the two-parameter Weibull distribution (Fig. 4)

$$P_f = 1 - \exp\left[- \left(\frac{\sigma_f}{S_o} \right)^m \right] \quad (15)$$

where S_o is the characteristic modulus of rupture and m is the Weibull modulus. The statistical material parameters S_o and m were determined by least-squares (LS) analysis and by the maximum likelihood method (ML). The results are shown in Table I. 90% confidence intervals were constructed where possible. The Kolmogorov–Smirnov test was used to determine the goodness of fit of the assumed distributions. The maximum deviation using the ML estimates ($m = 9.05$, $S_o = 12.27$ MPa) was 0.223 which corresponds to a probability of 39% of such a deviation occurring by chance. The corresponding numbers for the LS estimates ($m = 9.35$, $S_o = 12.27$ MPa) were 0.224 and 38%, respectively. Hence the parameter estimates were considered to be acceptable. The LS estimates are used in all subsequent analyses. The Weibull scale parameters, σ_{ov} ($= 2.47$ MPa m$^{0.32}$) of Equation 5 and σ_{os} ($= 3.71$ MPa m$^{0.32}$) of Equation 9, and the Batdorf coefficients, k_{BV} of Equation 11 and k_{BS}, were determined from S_o, m and the specimen geometry.

TABLE I Weibull parameters (Equation 15), confidence limits and Kolmogorov–Smirnov test results for vitrified alumina four-point bend bar fracture data

Method of Analysis	ML	LS
Weibull modulus, m	9.05	9.35
90% confidence limits on m (lower–upper)	5.79–11.75	–
Characteristic strength S_o (MPa)	12.27	12.26
90% confidence limits on S_o (lower–upper)	11.61–12.98	–
Kolmogorov–Smirnov test statistic	0.223	0.224
Significance level (%)	39	38

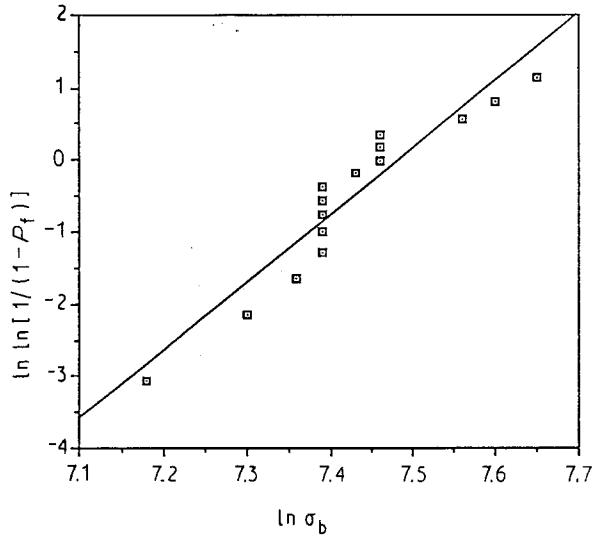

Figure 4 Weibull strength distributions of vitrified four-point bending bars of aluminium oxide.

Thirteen grinding wheels, from the same batch as used in the bend tests, were spin-tested to failure. These wheels had an outer diameter of 254 mm, an inner diameter of 85.7 mm and a thickness of 19 mm. The Weibull modulus (m) that characterized the spin-test fracture data was 10.02, which compares well with $m = 9.35$ (LS) from the bending strength data. The experimental probability of failure in the spin test is shown plotted against the spin speed in Fig. 5. Also shown in this figure are the predicted probabilities of failure in the spin test determined using the bend-strength data of Fig. 4. It was hard to establish from the fractured wheels as to whether fracture originated from a volume or a surface flaw. This was the case with the bend-strength specimens too. Because of this uncertainty, failure probabilities were computed separately for a critical volume flaw assumption (Fig. 5a) and for a critical surface flaw assumption (Fig. 5b).

Fig. 5a shows two computed failure curves alongside the experimental curve. The curve defined by square symbols was computed assuming (i) that fracture was caused by volume flaws and (ii) a shear-insensitive (Weibull approach) fracture criterion (Equation 3). The curve defined by triangular symbols was obtained with the shear-sensitive criterion of Batdorf (Equation 10) with σ_e defined by Equation 12. Fig. 5b shows the corresponding curves for the surface flaw assumption. Equation 7 was used to compute failure probabilities for surface flaw-dominated fracture with the Weibull approach and Equation 14 was used for the Batdorf (shear-sensitive) approach.

Sixteen wheels from the same batch as used earlier were loaded to failure using the internal pressure apparatus of Fig. 1. Fig. 6 shows the distribution of the experimental fracture pressures in a typical Weibull plot. The fracture pressures in Fig. 6 have been corrected for the 4 mm thick epoxy layer on the inner diameter of the grinding wheels. The same experimental data are presented as a failure probability curve in Fig. 7 (circular symbols). Fig. 7a also shows

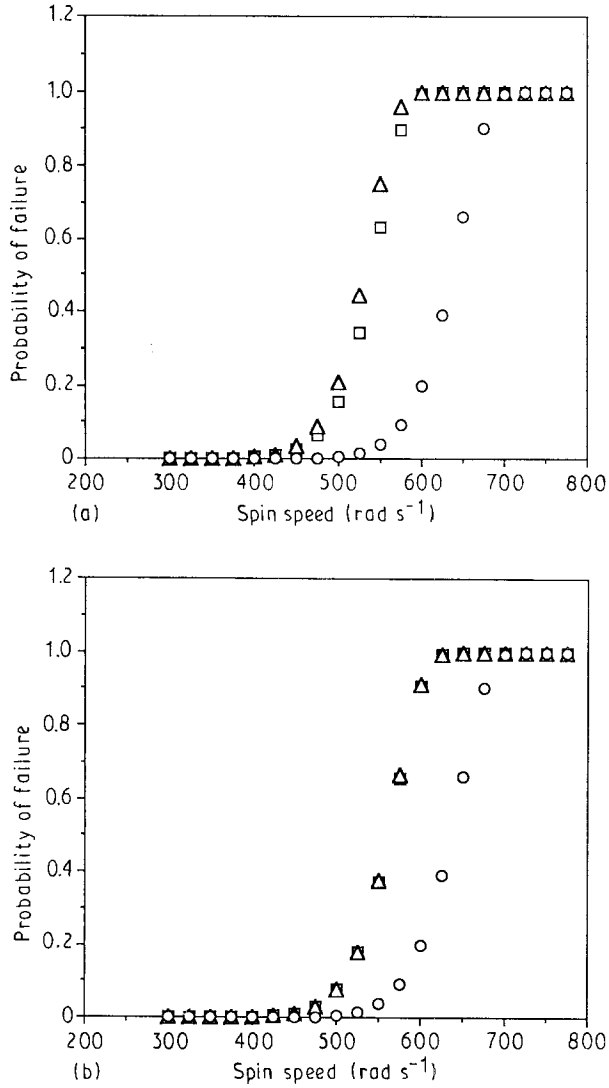

Figure 5 Comparison of experimental failure probabilities with predicted failure probabilities, using four-point bend-strength data, for grinding wheels subjected to the spin test: (a) volume flaw analysis, (b) surface flaw analysis. (□) Weibull approach, (△) Batdorf approach, (○) experimental.

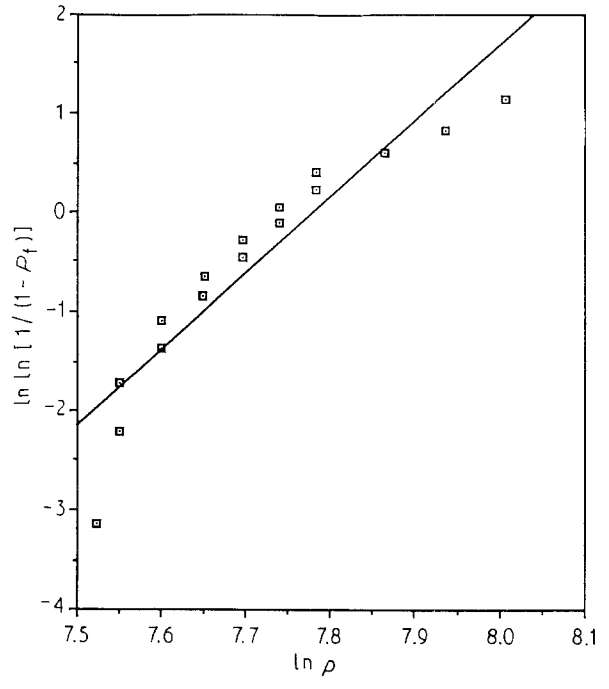

Figure 6 Weibull distribution of fracture pressures in internal pressure test.

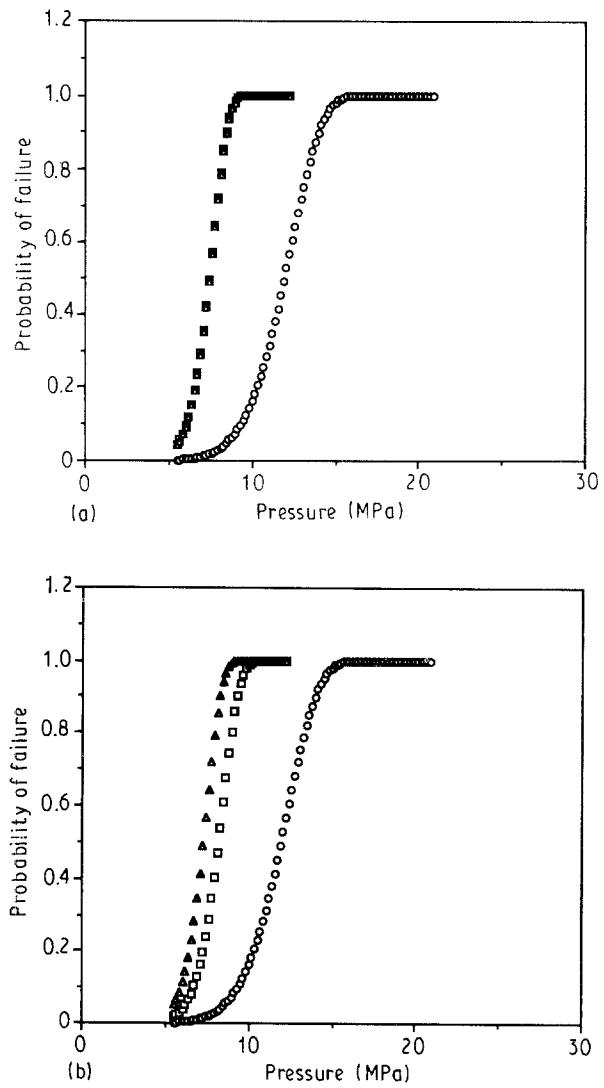

Figure 7 Comparison of experimental failure probabilities with predicted failure probabilities, using four-point bend-strength data, for failure in the internal pressure test: (a) volume flaw analysis, (b) surface flaw analysis. (□) Weibull, (△) Batdorf, (○) experimental.

failure probability curves for the internal pressure test, computed using bending-strength data and based on the assumption that volume flaws caused fracture. The results based on a surface-flaw assumption are presented in Fig. 7b.

From Figs 5a, 5b, 7a and 7b it is apparent that the difference between the predictions of the shear-insensitive and shear-sensitive criteria is minimal. The shear-sensitive criterion is slightly more conservative. From the figures it is also apparent that predictions based on the bending-strength data fall short of the experimental probability curves irrespective of the critical flaw type (volume or surface) assumption.

The foregoing analysis and figures have all been based on the crucial assumption that the bend bars and the grinding wheels have essentially the same strength-controlling flaw populations. It is quite likely that this assumption is erroneous. The bend bars were sliced from grinding wheels and were ground before being fractured. Each of these processes introduces defects that could change the nature of the flaw population. If that is the case, predictions of failure in the spin or the internal pressure test using bend-strength results will be erroneous. However, the wheels used in

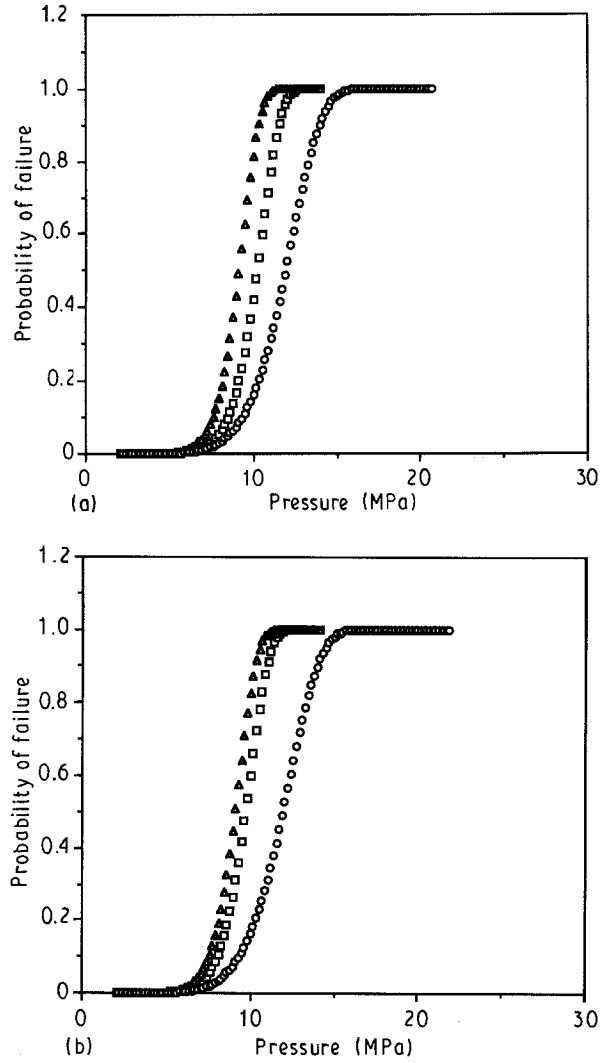

Figure 8 Comparison of experimental failure probabilities with predicted probabilities, using spin-test failure data, in the internal pressure test: (a) volume flaw analysis, (b) surface flaw analysis. (□) Weibull, (△) Batdorf, (○) experimental.

both the spin test and the internal pressure test were produced in the same batch and should therefore have the same flaw populations. Hence it should be possible to deduce flaw population characteristics (Weibull and/or Batdorf parameters) from spin-test fracture data and use these characteristics to predict failure in the internal pressure test. The results of such an analysis are shown in Fig. 8a (volume flaws) and Fig. 8b (surface flaws). The spin test does underpredict failure probabilities in the internal pressure test but the differences are not as extreme as in Figs 5 and 7.

One possible source for the disagreement is the fairly small sample sizes used in both tests (13 in the spin test and 16 in the internal pressure test). Another factor that contributes to the error is the epoxy coated on the insides of the wheels prior to subjecting them to the internal pressure test. As stated earlier, the epoxy is necessary to prevent leakage through the pores of the grinding wheel. While the experimentally measured pressures have been corrected to take into account the epoxy layer for estimating the true pressure acting at the inner wheel radius, the correction has been made on the assumption that the epoxy layer is of uniform thickness. In practice this is not the case. Given these potential sources of error it is reasonable to state that on the basis of the results in Fig. 8, failure in the spin test correlates reasonably well with failure in the internal pressure test. The experimental 50% failure pressure in the internal pressure test is within 15% of the predicted (from spin-test results) 50% failure pressure. This being the case, the internal pressure test can be used in lieu of the spin test to test grinding wheels. An equivalent "proof pressure" can be derived corresponding to a given "proof speed" in the spin test. The "proof pressure" will have the same probability of failure as the "proof speed" used in the spin test (usually 1.5 times the designed operating speed).

It should be emphasized that the internal pressure test does not require any destruction of or changes in the grinding wheel. It is true that a coating of epoxy was applied to the internal hub of the grinding wheel in the internal pressure test. In practice this need not be the case. We have constructed an internal pressure fixture consisting of a thin-walled diaphragm which can be inserted into the bore of the wheel. Pressure is applied to the bore wall by means of this diaphragm. The need for an epoxy coating is thus eliminated. Validation experiments to develop a standardized proof test using this new fixture are currently in progress.

4. Conclusions

The internal pressure test has been developed as an alternative to the spin test for testing fast-fracture reliability of grinding wheels. Four-point bend strength tests were used to characterize the flaw populations in the grinding wheels. These flaw populations were then used to predict failure in the spin test and the internal pressure test. The differences in the predictions based on shear-insensitive (Weibull) and shear-sensitive (Batdorf) criteria were found to be very small. The four-point bend strength data were found to underpredict failures in both tests, thus casting doubt on the assumption of identical flaw populations. However, failure probabilities in the internal pressure test, derived from the spin-test fracture data, were in reasonably good agreement with experimental results. Hence the internal pressure test is equivalent to the spin test for determining the fast-fracture reliability of grinding wheels. The internal pressure test is simple and economical (unlike the spin test) and can be performed by both wheel manufacturers and users. It does not require any destruction of or changes to the grinding wheel, especially when an internal metal/rubber diaphragm is used to apply the pressure to the hub of the wheel.

Acknowledgement

The authors wish to thank Ferro Electro Corporation, Buffalo, New York for providing the grinding wheels that were used in the study and for performing the spin tests at their facility.

References

1. J. E. RITTER and S. A. WULF, *Amer. Ceram. Soc. Bull.* **57** (1978) 186.

2. W. JOHNSON, Y. L. BAI and S. K. GHOSH, *J. Engng Mater. Technol.* **108** (1984) 167.
3. S. A. HAYWOOD, *Br. Ceram. Soc. Trans.* **83** (1984) 134.
4. R. L. SMITH, *Br. J. Non-Destr. Test* **28** (1986) 73.
5. S. KUMEKAWA, R. KOMANDURI and M. C. SHAW, in US Patent No. 4 137 516 (1977).
6. T. ISHIKAWA, MS thesis, Arizona State University (1981).
7. W. WEIBULL, *J. Appl. Mech.* **18** (1951) 293.
8. O. VARDAR and I. FINNIE, *Int. J. Fract.* **11** (1975) 495.
9. Y. MATSUO, *Bull. JSME* **22** (1979) 1053.
10. S. B. BATDORF and J. G. CROSE, *J. Appl. Mech.* **41** (1974) 459.
11. S. B. BATDORF and H. L. HEINISCH, *J. Amer. Ceram. Soc.* **61** (1978) 355.
12. T. H. SERVICE and J. E. RITTER, *J. Vibration, Acoustics, Stress, Reliabil. Design* **111** (1989) 194.
13. R. M. WILLIAMS and L. R. SWANK, *J. Amer. Ceram. Soc.* **66** (1983) 765.
14. N. N. NEMETH, J. M. MANDERSCHEID and J. P. GYEKENYESI, *Amer. Ceram. Soc. Bull.* **68** (1989) 2064.
15. H. FORD and J. M. ALEXANDER, *Advanced mechanics of MHS*, Longmans, London (1972), pp. 281–282.

Received 12 March
and accepted 1 July 1991